AIP | Journal of Applied Physics

Photoluminescence from single nitrogen isoelectronic centers in gallium phosphide produced by ion implantation

G. Éthier-Majcher, P. St-Jean, A. Bergeron, A.-L. Phaneuf-L'Heureux, S. Roorda et al.

Citation: J. Appl. Phys. **114**, 034307 (2013); doi: 10.1063/1.4815883
View online: http://dx.doi.org/10.1063/1.4815883
View Table of Contents: http://jap.aip.org/resource/1/JAPIAU/v114/i3
Published by the AIP Publishing LLC.

Photoluminescence from single nitrogen isoelectronic centers in gallium phosphide produced by ion implantation

G. Éthier-Majcher,[1] P. St-Jean,[1] A. Bergeron,[1] A.-L. Phaneuf-L'Heureux,[1] S. Roorda,[2] and S. Francoeur[1]
[1]*Département de génie physique, Polytechnique Montréal, Montréal H3C 3A7, Canada*
[2]*Département de physique, Université de Montréal, Montréal H3C 3J7, Canada*

(Received 24 May 2013; accepted 28 June 2013; published online 17 July 2013)

Single emitters formed from two nitrogen isoelectronic traps in GaP are created by low energy implantation. Several dyad configurations are individually resolved, establishing that ion implantation can produce multi-impurity single emitters with high luminescence yield. Measured dyad concentrations significantly exceed those predicted from simulations, suggesting that their formation is strongly enhanced by implantation defects. Annealing at 600 °C optimizes the luminescence yield and higher temperatures lead to the physical dissociation of dyads. The dissociation activation energy increases with interatomic separation, indicating that nearest neighbor dyads are energetically unfavorable and that their concentration can be adjusted with a simple temperature treatment. © *2013 AIP Publishing LLC*. [http://dx.doi.org/10.1063/1.4815883]

I. INTRODUCTION

Atomic systems embedded in solids, like nitrogen-vacancy centers in diamond and phosphorus impurities in silicon, have attracted much attention in recent years as promising candidates for the implementation of quantum information processing and single-atom electronic devices. A lesser known atomic system, isoelectronic centers in semiconductors, could be another suitable candidate offering advantageous characteristics for these applications. Formed by one or few isovalent impurities, these centers can bind excitons, charged excitons and biexcitons[1] and can be addressed electrically and optically. Their characteristics are reminiscent of both deep impurities and semiconductor quantum dots, making the physics governing their behavior intriguing and potentially profitable for the development of classical and quantum device functionalities. For example, their properties can be tailored, to a relatively large extend, by varying the number of impurities forming the center and the interatomic distance separating these impurities.

A number of isoelectronic centers composed of two isoelectronic traps, i.e., a dyad, have been optically resolved and individually studied: N dyads in GaAs,[2] AlAs,[3] and GaP[4] and Te dyads in ZnSe.[5] The samples used for these studies were produced by molecular beam epitaxy (MBE) or metal-organic chemical vapor deposition (MOCVD). These two approaches seldom offer the required control over the impurity concentration essential for the study of single emitters and are too often limited to elements for which the growth apparatus has been designed for or dedicated to. In contrast, ion implantation could be used to incorporate a variety of isoelectronic centers in a wide selection of host semiconductors, conveniently allowing the exploration of many impurity-host systems. Implantation of N in diamond and P in Si has been used to study single impurity centers[6,7] and to produce in these systems patterns with relatively high precision, a key requirement that will have to be addressed for quantum device fabrication. In this work, we demonstrate that ion implantation can be used to produce nitrogen dyads in GaP, that their concentration can be adjusted by a thermal anneal and that the obtained sample quality and luminescence yield allows to individually resolve and study dyads with several atomic configurations.

II. METHODS

N_2^+ ions are implanted at room temperature in high-quality GaP epilayers. A relatively low implantation energy of 20 keV/ion, corresponding to 10 keV per nitrogen atom, is used to minimize both the implantation damage and, due to a low straggle, the number of implanted ions necessary for achieving a given nitrogen dyad surface density. The optical resolution of our microluminescence system of 0.7 μm^2 sets the maximum surface dyad density that can be resolved (1.4 μm^{-2}). From this criterion, a target surface density of $C_s = 0.07\ \mu m^{-2}$ was selected.

This target surface density is used to determine the required ion fluence. A simulation using SRIM[8] gave a range $R_p = 25.5$ nm and a straggle $\Delta R_p = 13.3$ nm. The resulting volume concentration of nitrogen atoms as a function of depth is modeled by $C_v(z) = \frac{Q}{\Delta R_p \sqrt{2\pi}} \exp\left(\frac{-(z-R_p)^2}{2\Delta R_p^2}\right)$, where Q is the fluence. Assuming no mutual interactions between nitrogen atoms and a uniform N distribution over P sites, the probability for a given N atom to form a dyad is $P_{NN} = ax(1-x)^b$, where x is the fraction of anionic sites occupied by nitrogen, a the number of equivalent directions for a given pair orientation ($a = 12$ for NN_1, a dyad oriented along [110]) and b the number of nearest anionic sites occupied by P atoms ($b = 26$ for NN_1). C_s is obtained by multiplying this probability by $\frac{C_v}{2}$ and integrating over the depth of the sample. At low nitrogen concentration, $(1-x)^b \approx 1$ and

$$C_s = \frac{aQ^2}{8N_s \Delta R_p \sqrt{\pi}} \operatorname{erfc}\left(\frac{-R_p}{\Delta R_p}\right), \tag{1}$$

where N_S is the volume concentration of anionic sites. From this equation, a required fluence of $3.7 \times 10^{11}\,\mathrm{cm}^{-2}$ is calculated.

The implanted samples were high-quality 800 nm epilayers grown by MOCVD on undoped (001) GaP substrates. Four epilayers labelled S1, S2, S3, and S4 were prepared and implanted with fluences equal to, respectively, 1, 1/3, 1/9 and 1/27 of the target fluence.

To improve crystalline quality and activate nitrogen atoms, samples were successively annealed for 15 s at temperatures ranging from 400 to 950 °C under an Ar atmosphere. To minimize phosphorus evaporation, implanted samples were capped using a GaP sacrificial sample. After each anneal, samples were optically excited at 405 nm and photoluminescence (PL) spectra were acquired at 12 K.

III. RESULTS AND DISCUSSION

The low-temperature PL spectrum of the reference gallium phosphide epilayer before implantation is shown in Fig. 1. Nitrogen being a common background impurity in GaP, a relatively weak A-line, resulting from the radiative recombination of an exciton bound to a single nitrogen atom,[9] is observed at 2.317 eV. The feature labelled S corresponds to sulfur impurities and will not be discussed further.

After implantation and before annealing, no additional nitrogen related features were observed, indicating that the crystal quality was compromised even at these low implantation energy and fluence. However, following an anneal at 600 °C, the low-temperature PL spectrum of sample S1 is dominated by excitons bound to different nitrogen dyad configurations, as shown in Fig. 1. The intensity of the A-line, which is proportional to the nitrogen concentration, is about 1000 times that of the unimplanted epilayer and a number of LO and TO phonon replica can be identified at lower energy. In contrast to the spectrum from the reference epilayer, emission from several nitrogen dyads ($NN_{1,2,3,4,5}$) is readily observed in implanted samples, indicating that the luminescence could easily be activated with a rapid thermal anneal. Here, NN_i historically refers to two nitrogen atoms in the *i*th nearest neighbor position of the anionic sublattice,[9] though NN_2 was later attributed to a nitrogen triplet (a triad) in Ref. 10. The kinetics of dyads and triads under thermal annealing are not expected to be directly comparable, hence, NN_2 will not be discussed further.

The width of nitrogen related emissions extracted from ensemble measurements can be used to estimate the overall sample quality. Linewidths of 1 meV observed for NN_i are very similar to that of (1) GaP before implantation (see Fig. 1), (2) delta doped GaP layers grown by MOCVD,[11] and (3) nitrogen doped GaAs grown by MBE.[2] This comparison indicates that the implantation damage created at an energy of 10 keV per atom do not add to the inhomogeneous broadening of the emission after an anneal at 600 °C.

In the process of determining the optimal anneal temperature, it was found that the emission intensity of all nitrogen-bound excitons depends sensitively on the anneal temperature. Figure 2 shows an Arrhenius plot of the integrated intensity of the A-line, NN_1, NN_3, and NN_5 for sample S1. Averaged over more than 20 points on the surface of the sample, the plotted intensities should be representative of the crystallinity of implanted samples and the number of active nitrogen atoms and dyads.

The intensity profile of the A-line can be explained as follows. From 400 to 600 °C, the intensity increases as damages are being repaired and nitrogen atoms are being activated into substitutional sites. At 600 °C, most atoms are activated and the intensity remains constant up to 850 °C. In this temperature range, nitrogen diffusion could occur, but

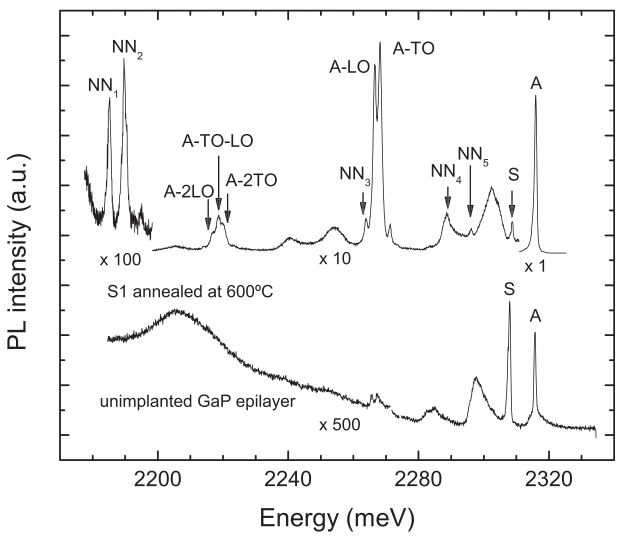

FIG. 1. PL spectra from the GaP epilayer before implantation and from sample S1 annealed at 600 °C. Lines A and S, respectively, correspond to emission from excitons bound to single nitrogen atoms and neutral sulfur donors, which are both present in the epilayer before implantation. Lines labelled NN_i correspond to emission from excitons bound to various nitrogen configurations. LO and TO are phonon replica of line A.

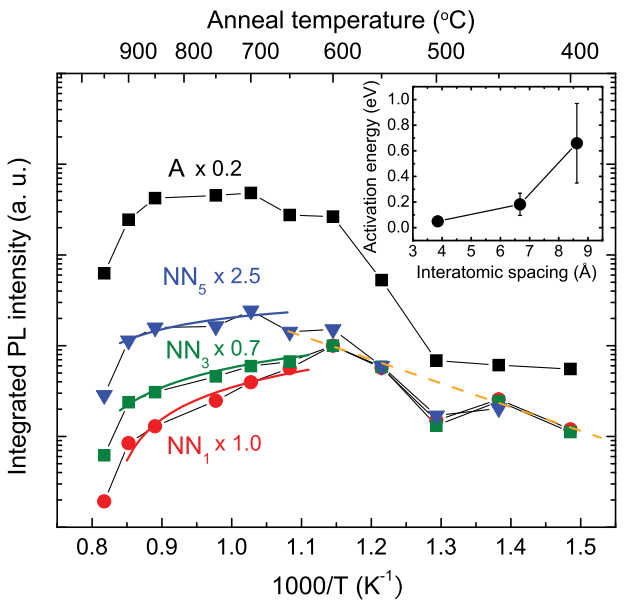

FIG. 2. Arrhenius plot of the integrated luminescence intensity of A, NN_1, NN_3 and NN_5 measured at 12 K for sample S1 after successive 15 s anneals at temperatures ranging from 400 to 950 °C. The measured intensities were multiplied by the normalisation factors shown. The dashed line is a fit of dyads activation energy and thick lines represent fitted intensities for the thermally activated dissociation of dyads. The inset shows the activation energies as function of the interatomic spacing of the dyads.

since the diffusion length is small compared to the optical excitation depth (~250 nm), diffusion does not affect the intensity of the A-line. Above 850 °C, the PL intensity decreases as phosphorus evaporation degrades the sample.

The temperature profiles of the PL intensity from NN_1, NN_3, and NN_5, normalized at 550 °C to allow for a better comparison, are also shown in Fig. 2. From 400 to 600 °C, the increase in intensity is identical for all three dyads and follows a thermally activated process with an activation energy fitted to 0.52 eV. This value is very close to 0.48 and 0.59 eV obtained in Refs. 12 and 13 for N implanted $In_{1-x}Ga_xP$, and to 0.50 eV reported in Ref. 14 for N implanted $GaAs_{1-x}P_x$. These energies were attributed to nitrogen atoms moving from interstitial to substitutional sites. At 600 °C, the intensity reaches a maximum and then decreases following an Arrhenius law, describing again a thermally activated process. Since the intensity of the A-line is constant in this temperature range, the creation of interstitial nitrogen or luminescence quenching defects are not expected to be important. This intensity reduction is therefore associated to the dissociation of nitrogen dyads. The intensities were fitted to $I = I_0(1 - e^{(-E_a/kT)})$, where E_a is the activation energy of the dissociation process. Interestingly, the activation energy varies significantly as a function of the atomic configuration: 0.05±0.03, 0.18±0.09 and 0.66±0.31 eV were found for NN_1, NN_3 and NN_5, respectively. Although NN_4 is present in Fig. 1, no dissociation energy could be extracted for this configuration because its emission energy coincides with a much more intense phonon replica of the A-line.

The activation energy of NN_1 being the lowest, it indicates that this dyad is easily dissociated and that forming a dyad of low interatomic separation is energetically unfavorable. The activation energies associated to NN_3 and NN_5 indicate that dyads of increasingly larger interatomic separation are more stable. Indeed, the intensity variation of NN_5 from 600 to 850 °C approaches that of the A-line, revealing that the concentrations of $NN_{i\geq 5}$ are not significantly affected by temperature in this temperature range. These results are consistent with deformation energy calculations suggesting that the formation of NN_1 in GaP is energetically unfavorable, while the energy balance of forming dyads of larger interatomic separation is more or less neutral.[15] Our results indicate that this transition is gradual and related to the dyad interatomic separation, as shown in the inset of Fig. 2. The dissociation process can therefore be used to reach concentrations of low interatomic separation dyads allowing single emitter studies with a simple temperature treatment.

Samples implanted at lower fluences showed a similar behavior under thermal annealing and, for all of them, the temperature optimizing PL intensity was about 600 °C. Samples implanted at higher energies (25 and 50 keV/atom), showed a lower luminescence yield, explained by the presence of unrecoverable damages.

Following an anneal at 600 °C, the emission from single nitrogen dyads was investigated. Microluminescence measurements were realized in a custom made confocal microscope[16] at 4 K. The 405 nm excitation illuminated the sample with a spot size of about 0.8 μm. The luminescence was collected through a single-mode optical fiber acting as a confocal aperture, resulting in a detection resolution also of 0.8 μm. A 750 mm spectrometer and CCD camera provided a spectral resolution of 125 μeV.

Figure 3 shows spatially resolved PL measurements at the emission energies of NN_3, NN_4, NN_5, and NN_7 from sample S4. These results clearly show that the PL is localized in an area of about 1 μm^2, which is defined by the spatial resolution of the measurement. The luminescence yield significantly exceeds the experimental background and instrumental noise, making it relatively easy to study the excitonic properties of individual emitters. Measurements on a large number of dyads only rarely revealed two dyads in the same detection volume, in which case, the two emitters could be easily discriminated through their polarization or their emission energy.

If implantation had resulted in a random distribution of nitrogen atoms, as assumed in the calculation of the target dose, it should have been possible to resolve nitrogen dyads in all four samples. However, surface concentrations of S1 and S2 were such that no dyads could be individually resolved. It is estimated that the actual dyad concentration is about 500 times higher than expected, indicating the presence of a mechanism enabling their formation. For example, divacancies on the phosphorus lattice produced during implantation could act as a precursor for the formation of dyads. Indeed, studies of implanted beryllium isoelectronic centers in silicon suggested that implantation defects facilitate the formation of dyads.[17] This beneficial effect reduces the nitrogen fluence necessary to achieve a given dyad concentration.

Figure 4 shows the polarization resolved luminescence of the NN_4 dyad shown in Fig. 3(b). Four excitonic transitions are associated to this dyad. In contrast to the linewidth of 1 meV obtained from ensemble measurements, the

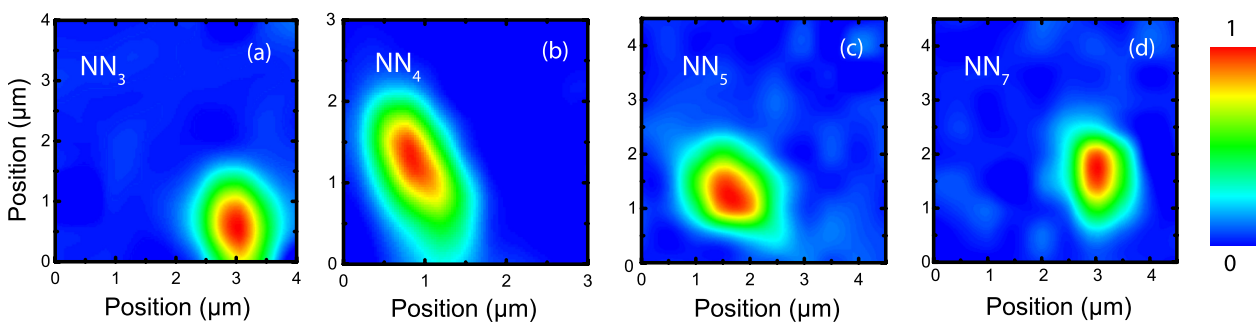

FIG. 3. Spatially resolved PL intensity from single nitrogen dyads taken at 4 K. The maps are acquired at (a) 2261.6 meV, (b) 2287.9 meV, (c) 2298.5 meV and (d) 2305.4 meV, corresponding to, respectively, NN_3, NN_4, NN_5, and NN_7.

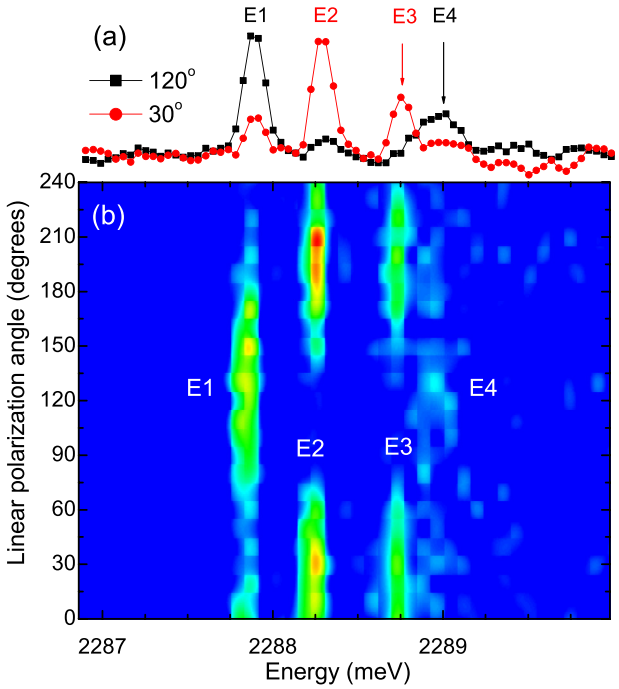

FIG. 4. (a) Polarization resolved PL spectra of a NN_4 dyad taken at 30 and 120° with respect to the [110] direction. Four linearly polarized transitions, labelled E1–E4 are observed. (b) Luminescence intensity from the same dyad as a function of the linear polarization angle and the energy.

linewidth of these transitions is limited by the spectral resolution of the instrumentation. Panel (b) shows the intensity as function of the linear polarization angle and PL energy. From measurements on large ensembles, the expected symmetry of NN_4 is C_{2v}.[9,18] When studying the emission from a single emitter, the orientational degeneracy is lifted and the excitonic fine structure observed depends on the orientation of the dyad with respect to $\hat{z}$, the direction of observation. If the dyad is positioned in the plane of the sample perpendicular to $\hat{z}$, four linearly polarized transitions with maxima along $\langle 110 \rangle$ should be observed. Otherwise, five linearly polarized transitions with maxima along $\langle 100 \rangle$ are expected.[19] Measurements on several NN_4 dyads with polarization angles along $\langle 110 \rangle$ (0 or 90°) or along $\langle 100 \rangle$ (45 or 135°) exhibiting the expected fine structure unambiguously confirm that the symmetry of this dyad is C_{2v}

For a few dyads, the polarization angles are not perfectly aligned with the expected axes. For example, the dyad shown in Fig. 4 exhibits polarization angles of approximately 30 and 120°. This deviation can be explained by the presence of a perturbation in the vicinity of the dyad,[19] produced by some impurity or crystallographic defect. Its precise nature is not known, but such perturbations are not necessarily related to implantation damage, as they have also been observed in samples grown by molecular beam epitaxy[19,20] and by chemical vapor deposition.[11]

IV. CONCLUSIONS

Considering the narrow emission linewidths observed, the high intensity contrast of linearly polarized emission lines, the statistics reconstructed from the measurement of a large number of dyads and the low implanted fluence, we conclude that single emitters are resolved, as it is statistically unlikely to obtain, in the same detection volume, two dyads with the same interatomic separation and oriented along the same crystallographic direction.[2]

Therefore, ion implantation can be used to produce low density centers composed of two isoelectronic traps that can be individually probed and studied. The current capability of resolving single emitters and studying their polarization selection rules should allow a rigorous determination of the exact atomic configuration associated to NN_i and resolving outstanding issues related to their energy ordering[15] and the number of nitrogen atoms involved.[10] Unrecoverable damages in the form of non-radiative centers and crystal disorder are not significant at low implantation energy, establishing ion implantation as a practical technique for the exploration of a large number of isoelectronic traps in a large variety of host materials.

ACKNOWLEDGMENTS

The authors thank C. Ouellet-Plamondon and S. Marcet for their early participation to this work and CMC Microsystems.

[1]S. Marcet, C. Ouellet-Plamondon, G. Éthier-Majcher, P. Saint-Jean, R. André, J. Klem, and S. Francoeur, Phys. Rev. B **82**, 235311 (2010).
[2]S. Francoeur, J. F. Klem, and A. Mascarenhas, Phys. Rev. Lett. **93**, 067403 (2004).
[3]M. Jo, T. Mano, T. Kuroda, Y. Sakuma, and K. Sakoda, Appl. Phys. Lett. **102**, 062107 (2013).
[4]M. Ikezawa, Y. Sakuma, and Y. Masumoto, Jpn. J. Appl. Phys., Part 2 **46**, L871 (2007).
[5]A. Muller, P. Bianucci, C. Piermarocchi, M. Fornari, I. C. Robin, R. André, and C. K. Shih, Phys. Rev. B **73**, 081306 (2006).
[6]J. Meijer, B. Burchard, M. Domhan, C. Wittmann, T. Gaebel, I. Popa, F. Jelezko, and J. Wrachtrup, Appl. Phys. Lett. **87**, 261909 (2005).
[7]D. N. Jamieson, C. Yang, T. Hopf, S. M. Hearne, C. I. Pakes, S. Prawer, M. Mitic, E. Gauja, S. E. Andresen, F. E. Hudson, A. S. Dzurak, and R. G. Clark, Appl. Phys. Lett. **86**, 202101 (2005).
[8]The simulation were realized using the SRIM group of programs calculating the stopping and range of ions in matter.
[9]D. G. Thomas and J. J. Hopfield, Phys. Rev. **150**, 680 (1966).
[10]B. Gil and H. Mariette, Phys. Rev. B **35**, 7999 (1987).
[11]M. Ikezawa, Y. Sakuma, M. Watanabe, and Y. Masumoto, Physica Status Solidi C **6**, 362 (2009).
[12]C. W. Chen and M. C. Wu, J. Appl. Phys. **72**, 1769 (1992).
[13]A. Fujimoto, Y. Makita, H. Nojiri, T. Kanayama, T. Tsurushima, and J.-i. Shimada, J. Appl. Phys. **51**, 3987 (1980).
[14]R. E. Anderson, D. J. Wolford, and B. G. Streetman, J. Appl. Phys. **48**, 2453 (1977).
[15]P. R. C. Kent and A. Zunger, Phys. Rev. B **64**, 115208 (2001).
[16]S. Marcet, C. Ouellet-Plamondon, and S. Francoeur, Rev. Sci. Instrum. **80**, 063101 (2009).
[17]T. G. Brown and D. G. Hall, in *Light Emission in Silicon: From Physics to Devices*, Semiconductors and Semimetals, edited by D. J. Lockwood (Elsevier, 1997), Vol. 49, pp. 77–110.
[18]B. Gil, J. Camassel, J. P. Albert, and H. Mathieu, Phys. Rev. B **33**, 2690 (1986).
[19]C. Ouellet-Plamondon, S. Marcet, J. Klem, and S. Francoeur, J. Lumin. **131**, 2339 (2011).
[20]D. Karaiskaj, A. Mascarenhas, J. Klem, K. Volz, W. Stolz, M. Adamcyk, and T. Tiedje, Phys. Rev. B **76**, 125209 (2007).